

# Digitally Controllable Large-Scale Integrated Microfluidic Systems

Raymond H. W. Lam, Kin Fong Lei, Josh H. M. Lam and Wen J. Li\*

Centre for Micro and Nano Systems  
The Chinese University of Hong Kong  
Hong Kong SAR

\*wen@acae.cuhk.edu.hk

**Abstract**—Active microfluidic mixers, micro vortex pumping devices, tesla microvalves, and microchannels were successfully fabricated using a single polymer based micro-molding process. These individual microfluidic devices were then integrated to perform precise fluid delivery, cutting, and mixing. Continuous and discretized pumping of fluids in microchannels can be achieved by the vortex micropumps that use rotating impellers. The fluid mixing is based on the vertical mechanical vibration of membranes driven by PZT actuator. Tesla microvalves were built to eliminate the backward flow by increasing the unidirectional back pressure. Experiments were conducted to investigate the performance of the mixing, pumping, and valving systems. The large-scale integration of microfluidic components using our micropump, microvalve and micromixer is also described in this paper.

**Keywords**—microfluidic system; microfluidic large-scale integration; micropump; micromixer; microvalve

## I. INTRODUCTION

A Microfluidic system is defined as a system composed of one or more of the various microfluidic devices. Micropump [1]–[3], microvalve [4]–[5], micromixer [6]–[7], microneedle [8] and microfluidic flow sensor [9] are some of the key microfluidic devices. In the past decades, researchers have contributed to both of the implementation and theoretical analyses [10]–[12] on each device. With the superior performance of the maturing microfluidic devices, the integration of microfluidic devices becomes the next challenge of the microfluidic technology. We will present in this paper our development of a technology to integrate many microfluidic components into a complex large-scale microfluidic system.

Research in microfluidic device has been an essential branch of the micro-electromechanical systems (MEMS) field. Initial microfluidic devices were mostly silicon-based. With the integrated circuit (IC) fabrication technology, microfluidic devices could have complicated structures and multiple layers. Device materials became an important issue since microfluidic devices were used in the bio-optical detection applications. The structural material of microchambers and microchannels is necessary to be transparent, chemically inactive and biocompatible, e.g., chemical reactions between structural material and fluid sample will affect the sample properties and should be

avoided. Polymer has been a vital material in microfluidic devices since it fulfills the above criteria, especially in bio-optical detection applications.

In most microfluidic systems, the micropump is an actuator that provides pressure to pump fluid into the system. The lead zirconate titanate (PZT) valveless micropump [7] is one of the conventional micropumps. In the design of a micropump, the main concerns are its occupied area, the applied voltage (or power), the flow rate induced and how much back pressure it can overcome. Some of the micropumps attain flow rates up to 1 ml/min and some are able to work against a back pressure higher than  $10^5$  Pa [13]. However, for practical applications, these performance parameters need to be further improved. Hence, the development of a small, low required voltage and high flow rate micropump can highly improve the applicability of microfluidic systems.

On the other hand, for more complicated microfluidic systems, mixing of more than one fluid is often required. Mixing of fluids is affected by the diffusion rate and the turbulence of fluid flow. Micromixer is used to enhance the mixing rate of fluid. The first micromixer used four hundred micronozzles inside a microchamber to increase the fluid diffusion rate [14]. This micromixer is defined as a passive micromixer since no external energy was used to induce the turbulence of fluid flow and enhance the mixing rate of fluid. The first active micromixer was reported by Zhen et al. [7]. An active micromixer can provide adjustable mixing rate, so it is more flexible in microfluidic applications.

The microfluidic systems for bio-optical detection applications involve fluid transmission, fluid multiplexing, fluid mixing, temperature and electrical potential controls, etc. Some of the applications require complicated microfluidic systems, so designing microfluidic chips for specific applications may not be a cost effective approach. Recently, a large-scale integrated microfluidic systems comprising of valves and channels using multiplayer soft lithography was developed by Quake's group [15]. They demonstrated microfluidic chips consisted of thousands of microvalves and hundreds of microchambers, which can potentially perform multiple bio-optical detection tasks. However, due to the fabrication process limitations, they could not integrate pumps or mixers onto their chips.

In this paper, we will present a system composed of microchannels, vortex micropumps, active micromixers and tesla microvalves, which can all be fabricated using a basic technology. The fabrication and operation principle of each device will be described. Experiments were conducted to test the performance of the integrated components of the system. Further large-scale integration of the mixing and pumping components will also be discussed.

## II. VORTEX MICROPUMP

The vortex micropump was fabricated using a micro molding replication technique developed by our group. Details of its working principle and characteristics are given in [16]. It was designed for microfluidic applications that require micro-liter delivery (see photograph in Figure 1). The dimension of the micropump module is 35 mm × 20 mm. The micropump has a pump chamber with 5 mm diameter. A 4 mm diameter impeller fabricated by electroplating is placed inside the chamber. Fluid can be pumped through a microchannel with 300 μm width and 150 μm depth. Since microfluidic devices are required to be transparent for bio-optical detection applications, so polymethyl methacrylate (PMMA) was chosen to be the structural material to build our vortex micropump. The micropump consists of two layers of patterned structure. The pattern on the lower layer includes a pump chamber and a microchannel fabricated by hot embossing process, while the upper layer is a cover layer providing an inlet and an outlet.

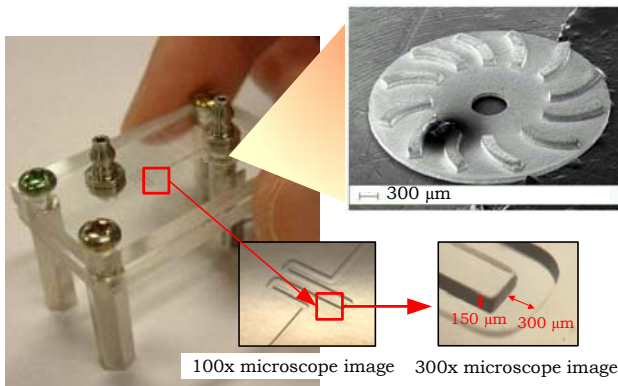


Figure 1. Photograph of a vortex micropump and its impeller and channel structure [16].

Continuous pumping can be achieved by the vortex micropump. The micropump converts the kinetic energy of an impeller to fluid movement. When fluid enters the chamber near the center of the impeller, the rotational motion of the impeller, driven by a DC motor, can induce fluid pressure by centrifugal force. Since the fluid pumping is based on the rotation of the impeller, the flow rate can be controlled by the input voltage. Experimental result indicates the flow rate is linearly proportional the applied voltage. The flow rate can achieve 2.45 ml/min at 3 V input voltage, and a pumping pressure of 7105 Pa at 2 V can be generated [16].

## III. FLAT-SURFACE DIAPHRAGM ACTIVE MICROMIXER

### A. Operation and Design

The flat-surface diaphragm (FSD) active micromixer consists of a PMMA substrate, a polyester layer, a metallic diaphragm and a piezoelectric lead zirconate titanate (PZT) ceramic. The pattern with depth of 80 μm contains a mixing chamber with 11 mm diameter, two 300 μm wide inlet channels and a 600 μm wide outlet channel. The profile of the patterned PMMA substrate is illustrated in Figure 2. Fluids from the two inlets will be merged into a single channel and enter the mixing chamber. The mixing chamber is for the enhancement of fluid mixing. The mixed fluids will eventually pass to the outlet after full mixing occurs.

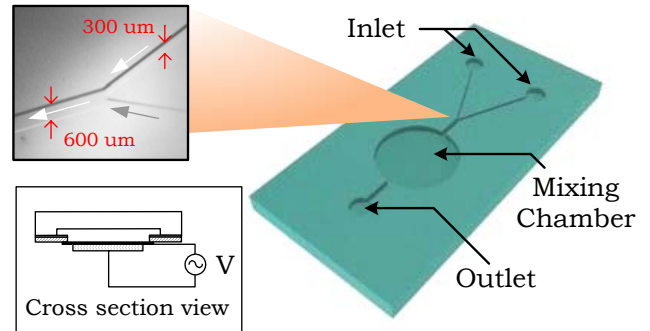


Figure 2. Pattern on the PMMA substrate and cross section view of the fluid chamber.

The operation of the FSD active micromixer is based on the mechanical vibration generated by the PZT ceramic. When two channels of fluid flow into a single channel, the fluid mixing inside the merged channel is insignificant because of the low diffusion rate, comparing to the flow rate. In the design of our micromixer, the mixing chamber, which contains an oscillating diaphragm, acts as an active microfluidic mixing component. When voltage is applied with the same direction of the poling field, the PZT ceramic will contract laterally, and vice versa. When a square wave signal is applied to the PZT film, the residual stress will cause the metallic diaphragm to vibrate horizontally. It has been shown that the vibration can enhance fluid mixing [7]. In our current work, a polymer based micromixer component is developed based on this principle.

A cross-section view of the mixing chamber is shown in Figure 2. A circular brass layer, with 13 mm diameter and 100 μm thickness, is bonded with the pattern side of the PMMA substrate. A piezoelectric PZT ceramic, with 9 mm diameter and 20 μm thickness, adheres to the brass layer. The PZT ceramic can be driven by a signal generator and a power amplifier to provide the mechanical oscillation. The resonant frequency of a silicon-based micromixer was obtained with 60 V peak-to-peak square wave at a frequency of 60 kHz [7].

## B. Fabrication

The fabrication process of the FSD active micromixer is illustrated in Figure 3. PMMA substrate is used because of its biocompatibility. The wall of channels and chamber is patterned by photolithography. MicroChem™ SU-8 2075 photoresist was spun on the substrate at 3000 rpm rotational speed. After soft bake at 65 °C for 5 mins and 80 °C for 40 mins, the SU-8 layer should be exposed under the mask with the channels and chamber pattern for 60 s. Post expose should be performed at 50 °C for 30 mins. The baked SU-8 should then be immersed in MicroChem's SU-8 Developer for 60 mins at room temperature. The channels and chamber profile could be obtained after brief rinse with isopropyl alcohol (IPA) and DI water. The inlets and outlet can be made by drilling holes with diameter 2.8 mm at the pattern terminals to allow the insertion of faucets. Then a polyester film, with a 10 mm diameter hole, should be bonded with the substrate using a layer of UV-curing epoxy resin, spun on at 4,000 rpm for 40 s. After UV-exposure, the closed channels can be built between the substrate and the film. Then the brass diaphragm can be bonded around the hole of polyester layer. Since a PZT ceramic layer is adhered under the diaphragm, the region below the mixing chamber could provide the mechanical oscillation of fluid. The upper and lower sides of the PZT ceramic are connected with electrical wires to receive the driving voltage.

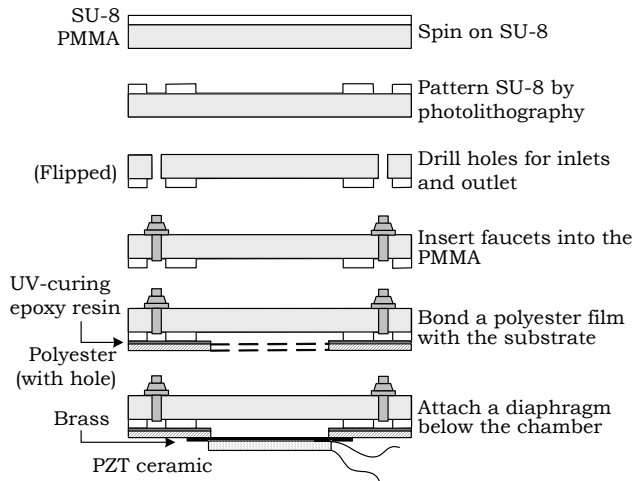


Figure 3. Simplified fabrication process of the micromixer.

A photograph of the fabricated micromixer is shown in Figure 4. Red ink was inserted inside the channel to illustrate the pattern of fluid flow. After the sample was cut by a diamond saw, the cross-section view of the 600  $\mu\text{m}$  wide microchannel was captured by the microscope with 250X magnification. Another 100X microscope image was captured at the merging region of the fluid. It indicates the UV-curing resin can provide a satisfying bonding profile. A biocompatible micromixer can be achieved by spinning a 40  $\mu\text{m}$  layer of silicone elastomer polydimethylsiloxane (PDMS) on the brass diaphragm.

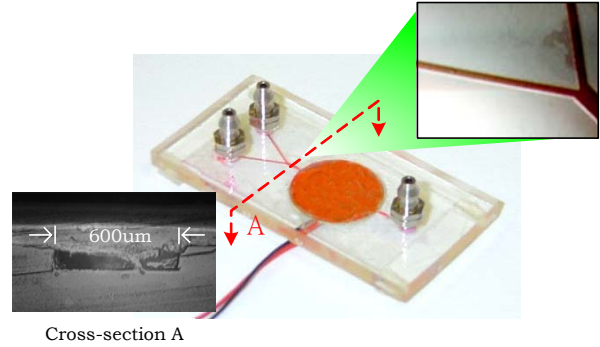


Figure 4. Photograph of the micromixer and microscope images of the channel features.

## IV. LARGE-SCALE INTEGRATED MICROFLUIDIC SYSTEMS

### A. Microfluidic Mixing System

A microfluidic mixing system was integrated as shown in Figure 5 (a). Two vortex micropumps were connected to the FSD active micromixer with 2.0 mm internal diameter tubes (Figure 5 (b)). A dual-output power supply was used to drive the micropumps. The working voltages of the micropumps were 0.4 – 3 V. To illustrate the mixing performance, two fluids with different colors (water and red ink) were chosen as solution entering through the inlets. After the two fluids merged into a single channel, they did not mix up because of insufficient diffusion rate. In the mixing chamber, the mechanical vibration of the piezoelectric diaphragm was used to enhance mixing rate. The voltage input of the diaphragm was produced by a signal generator and a power amplifier. The mixed fluid was passed to the outlet eventually (Figure 5 (c)).

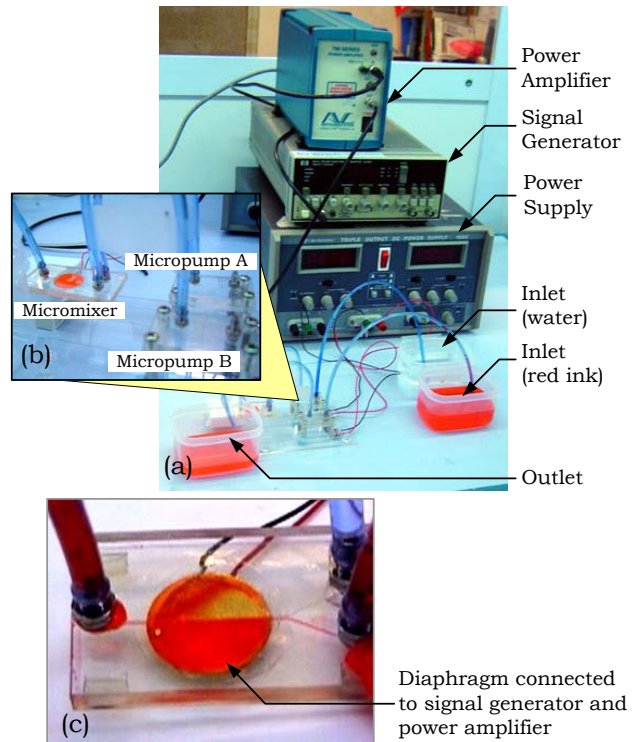


Figure 5. Experiment configuration of the integrated mixing system.



In the experiment, both micropumps were driven by 0.9 V input voltage. When fluids were passed into the chamber, they could not mix up because of the continuous flow rate as shown in Figure 6 (a). A sharp and straight interfacial line between water and red ink indicated the balanced pump pressure between the two micropumps. We started to applied square wave signal to the FSD active micromixer at 10 s. The mechanical vibration greatly enhanced the mixing rate inside the chamber (Figure 6 (b)). The resonant frequency of the diaphragm could be obtained with 55 V peak-to-peak bipolar square wave voltage at a frequency of 0.9 kHz. The typical time for thorough mixing was about 1 min (Figure 6 (c)). The thorough mixing could be retained with unchanged signal frequency. After we turned off the signal generator at 1 min 20 s, the fluid inside the chamber was reverted to be half red and half transparent. The typical restoring time was around 1 min 30 s (Figure 6 (d) – (e)). At 4 min 0 s, the input signal was applied to the micromixer again. Then the input signal was turned off at 5 min 5 s. Repeatable results could be obtained in our experiment (Figure 6 (f) – (i)). Besides, the time for thorough mixing and restoring were still 1 min and 1 min 30 s, respectively.

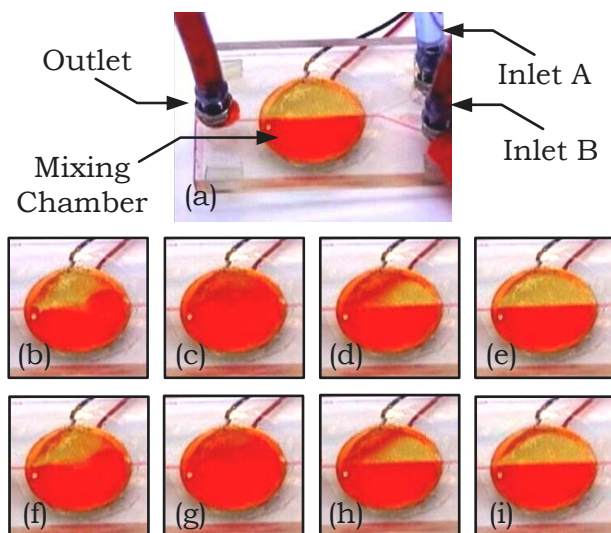


Figure 6. Fluid inside mixing chamber during experiment at (a) 0 s, (b) 20 s, (c) 1 min 10 s, (d) 1 min 47 s, (e) 2 min 55 s, (f) 4 min 18 s, (g) 5 min 5 s, (h) 5 min 45 s and (i) 6 min 40 s.

### B. Mixing Rate Enhancement

In the current microfluidic mixing system, the time for thorough mixing is about 1 min. The duration is a significant factor in some microfluidic applications. For passive micromixers, mixing is enhanced by adding pillars inside the chamber. Hence, integrating the pillars and vibrating diaphragm is a potential technique to further improve the mixing duration.

A pillared-surface diaphragm (PSD) active micromixer, which combines the mixing elements in both active and passive micromixers, was developed. The chamber profile of a fabricated PSD active micromixer is illustrated in Figure 7. Pillars with dimensions  $500\ \mu\text{m} \times 500\ \mu\text{m} \times 80\ \mu\text{m}$  was evenly distributed inside the chamber (Figure 7 (a) and (b)). The wall of the chamber and microchannels was  $160\ \mu\text{m}$  in height (Figure 7 (c)). The fabrication of the PSD

active micromixer was the same as the active one except for the photolithography process. The PSD active micromixer used double layer of SU-8 to create a more complicated geometry. The photolithography process of the PSD active micromixer is shown in Figure 8. Pillars were created on the topside of the mixing chamber. The height of the chamber wall was twice that of the pillars, so the diaphragm could vibrate freely under the chamber.

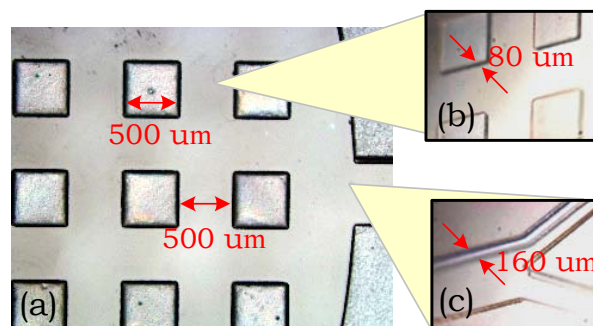


Figure 7. (a) Top view of mixing chamber and (b) isometric views of pillars and (c) microchannels.

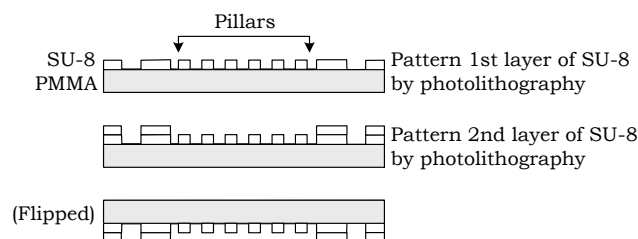


Figure 8. Simplified lithography process of the PSD active micromixer.

An Experiment was performed to verify the mixing performance of the PSD active micromixer. The experimental setup was the same as the one shown in Figure 5 except for the micromixer and the variation of the input frequency. The FSD active micromixer was replaced with the PSD active micromixer, which was driven with 55 V peak-to-peak bipolar square wave voltage at a frequency of 1.4 kHz. The fluid pattern inside the chamber during experiment is shown in Figure 9. The mixing time was about 5 s (Figure 9 (a) – (c)) and the restoring time remained 1 min 30 s (Figure 9 (c) – (e)). Moreover, the results are reproducible (Figure 9 (e) – (i)). This demonstrated that adding pillars inside the mixing chamber could help further induce significant improvement on the fluid mixing.

The input voltage frequency is also an important factor for the mixing performance, other than the chamber geometry. The relationship between the mixing time and the input voltage frequency was investigated experimentally. The mixing time of the FSD and PSD active micromixers for different input voltage frequencies is shown in Figure 10. Thorough mixing occurred when the input frequencies are greater than 0.6 kHz and 0.5 kHz for the FSD and PSD active micromixers, respectively. For input frequency greater than 9 kHz, the mixing enhancement by the diaphragm vibration became insignificant. The experimental result indicates that the pillars could further shorten the required mixing time. The

optimal mixing time of the FSD active micromixer was 60 s at a frequency of 0.9 kHz, and the optimal mixing time of the PSD active micromixer was 2 s at a frequency of 1.5 kHz.

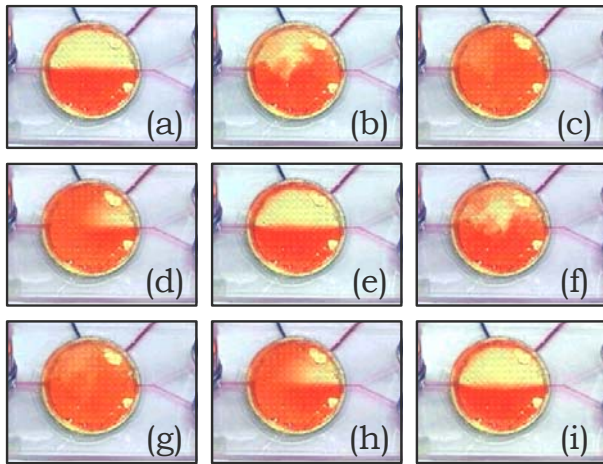


Figure 9. Fluid inside the mixing chamber of the PSD active micromixer during experiment at (a) 0 s, (b) 1 s, (c) 5 s, (d) 15 s, (e) 95 s, (f) 97 s, (g) 100 s, (h) 111 s and (i) 176 s.

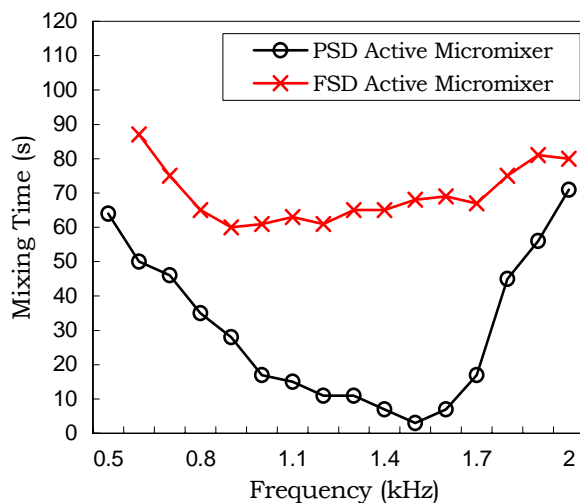


Figure 10. Mixing Time of the FSD and PSD active micromixers corresponding to different input frequencies.

### C. Backward Flow Elimination by Tesla Valves

In the microfluidic systems with multiple micropumps, fluid pumping of a micropump can induce backward fluid flow in other pump channels. A typical example is a “Y”-shape microchannel with two micropumps as illustrated in Figure 11. To eliminate the interference of the pressure between different micropumps, tesla valves can be added at the inlet channels. The working principle of tesla valve is shown in Figure 12 (a). When micropump B is on and micropump A is off, backward flow pressure will be induced in the pump channel of micropump A. Since the geometry of the tesla valve causes a high back pressure along pump channel A, the backward flow can be eliminated.

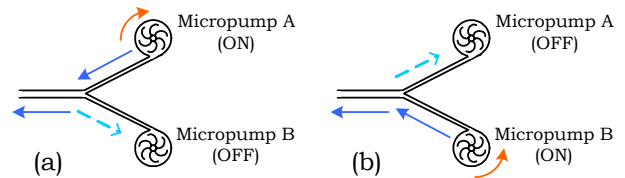


Figure 11. Backward fluid flow in “Y”-shape microchannel. (a) The pumping pressure of micropump A causes backward flow in pump channel B, and (b) vice versa.

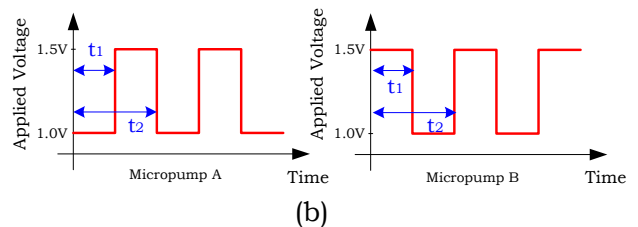
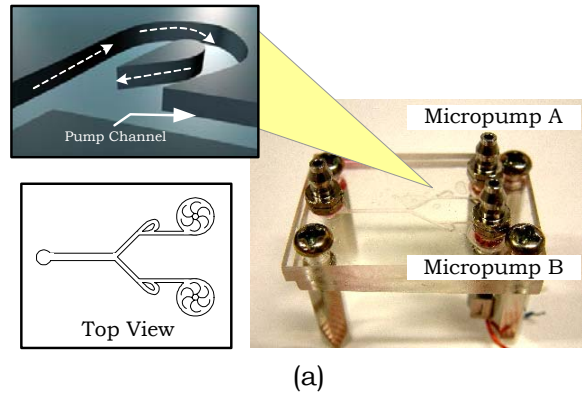


Figure 12. (a) Schematic drawing of tesla valve and (b) time sequence of applied voltage of the two micropumps.

A micropumping system integrated with two micropumps, two tesla valves and a “Y”-shape channel was built and tested. The tesla valves prevented backward flow and retained the flow rate of micropumps. With the applied voltage sequence shown in Figure 12 (b), fluids can be swapped in the flow channel. The proportion of the two fluids was controlled by the duty cycle  $t_1$ . That is, discretized fluid mass can be delivered in the channel using this technique. The accuracy of the flow rate and the fluid mass delivered could be greatly improved by the digitally controllable micropumping system described above.

### D. Digitally Controllable Microfluidic Mixing System

The digitally controllable micropumping system described in this paper can provide accurate and discretized fluid flow. Multiple fluids with variable proportion can also be pumped with digital input voltage. The microfluidic mixer uses square wave input voltage to actuate the diaphragm vibration. Therefore, a digitally controllable microfluidic mixing system can be integrated from the mixing and pumping devices. The proposed system consists of an array of digitally controllable microfluidic mixing module as illustrated in Figure 13. In each mixing module, a chemical is pumped into an inlet, while another inlet is filled with DI water (or any given solution). Concentration of chemical is adjustable by different pumping rate of the vortex micropumps. The tesla

microvalves are used to prevent the backward flow and the chemical diluting with water. The mixing of the chemical and water is insignificant in the microchannel due to very low Reynold's number for the flow. The mixing chamber can then enhance the fluid mixing, and so a specific chemical with desirable concentration can be obtained at the outlet of each mixing module.

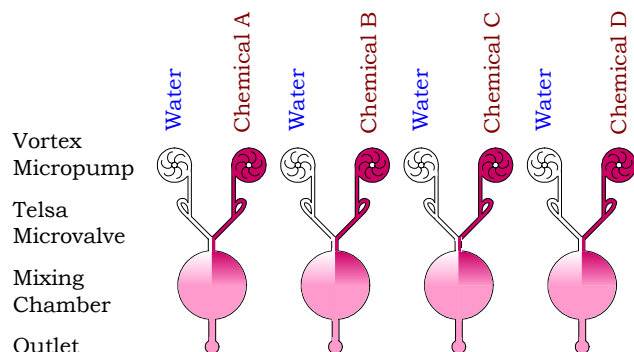


Figure 13. Schematic drawing of an array of digitally controllable microfluidic mixing modules.

With an array of digitally controllable mixing modules, multiple chemicals with different concentrations can be generated. Preparation of chemical samples is requisite in most of the microfluidic systems. Combining the mixing system with other microfluidic chips, less bulky macro-equipment is required and the integrated system will become much more portable. The on-chip chemical batch preparation reduces the necessary inlets and outlets for fluid connections. Consequently, it enables more complicated design of microfluidic system.

## V. CONCLUSION

The polymer-based vortex micropump, active micromixers and tesla microvalve were developed and integrated into a microfluidic system capable of delivering discrete fluid masses and mixing solutions. The flow rate of the vortex micropump is proportional to the applied voltage. The driving voltage is 0.4 V – 3 V. The flow rate and the pumping pressure of the micropump can achieve 2.45 ml/min at 3 V and 7105 Pa at 2 V, respectively. The FSD active micromixer can encourage a significant mixing with 55 V peak-to-peak bipolar square wave input voltage at a frequency of 0.9 kHz. The microfluidic mixing system was integrated with two vortex micropumps and an FSD active micromixer. The mixing time is 1 min and the restoring time is 1.5 mins. A PSD active micromixer with pillars inside the mixing chamber was developed. Experiments were also performed to show adding pillars could further shorten the mixing time to be <5 s. A tesla valve that eliminates backward flow by increasing the back pressure of the inactive pump channels was also designed and built. A microfluidic pumping system consisted of two vortex micropumps, two tesla valves and a “Y”-shape channel was also developed. Swapping of discretized fluid supply can be obtained at the outlet. The proportion between two inlet fluids can be also adjustable with different pumping duty cycles. Due to the planar geometry of vortex micropump, active micromixers and tesla

microvalve, a digitally controllable mixing system on a biocompatible polymer substrate can be potentially integrated to perform complex sample preparation, chemical analyses, fluid delivery, DNA detection, etc. In essence, we have demonstrated a technology that can be extended to build large-scale integrated microfluidic system.

## REFERENCES

- [1] R. Linnemann, P. Woias, C.-D. Senfft and J. A. Ditterich, “A self-priming and bubble-tolerant piezoelectric silicon micropump for liquids and gases,” *Proceedings of Micro Electro Mechanical Systems 1998 (MEMS 98)*, pp. 532-537, 1998.
- [2] Chaun Hua Chen and J. G. Santiago, “A planar electroosmotic micropump,” *Journal of Microelectromechanical Systems*, vol. 11, pp. 672-683, 2002.
- [3] Yo Han Choi, Son Sanguk and S. S. Lee, “Novel micropump using oxygen as pumping source,” *Proceedings of Micro Electro Mechanical Systems 2003 (MEMS 03)*, pp. 116-119, 2003.
- [4] Marc A. Unger, Hou-Pu Chou, Todd Thorsen, Axel Scherer and Stephen R. Quake, “Monolithic Microfabricated Valves and Pumps by Multilayer Soft Lithography,” *Science*, vol. 288, pp. 113-116, 2000.
- [5] N. Vandelli, D. Wroblewski, M. Velonis and T. Bifano, “Development of a MEMS microvalve array for fluid flow control,” *Journal of Microelectromechanical Systems*, vol. 7, pp. 395-403, 1998.
- [6] Hsin Yu Wu and Cheng Hsien Liu, “A novel electrokinetic micromixer,” *Transducers, Solid-State Sensors, Actuators and Microsystems*, vol. 1, pp. 631-634, 2003.
- [7] Z. Yang, M. Matsumoto and H. Goto, R. Maeda, “Ultrasonic micromixer for microfluidic systems,” *Sensors and Actuators*, vol. 93, pp. 266-272, 2001.
- [8] J. D. Zahn, A. A. Deshmukh, A. P. Pissano and D. Liepmann, “Continuous on-chip micropumping through a microneedle,” *Proceedings of Micro Electro Mechanical Systems 2001 (MEMS 01)*, pp. 503-506, 2001.
- [9] Gerlinde Bedö, Heike Fannasch and Rudolf Müller, “A silicon flow sensor for gases and liquids using AC measurements,” *Sensors and Actuators*, vol. 85, pp. 124-132, 2000.
- [10] Shifeng Li and Shaochen Chen, “Analytical analysis of a circular PZT actuator for valveless micropumps,” *Sensor and Actuator*, vol. 104, pp. 151-161, 2003.
- [11] A. Bertsch, S. Heimgartner, P. Cousseau and P. Renaud, “3D micromixers-downscaling large scale industrial static mixers,” *Proceedings of Micro Electro Mechanical Systems 2001 (MEMS 01)*, pp. 507-510, 2001.
- [12] S. D. Muller, I. F. Sbalzarini, J. H. Walther and P. D. Koumoutsakos, “Evolution strategies for the optimization of microdevices,” *Proceedings of the 2001 Congress on Evolutionary Computation*, vol. 1, pp. 302-309, 2001.
- [13] J. C. Rife, M. I. Bell, J. S. Horwitz, M. N. Kabler, R. C. Y. Auyeny and W. J. Kin, “Miniature valveless ultrasonic pumps and mixers,” *Sensors and Actuators*, vol. 86, pp. 135-140, 2000.
- [14] R. Miyake, T. S. J. Lammerink, M. Elwenspoek and J. H. J. Fluitman, “Micromixer with fast diffusion,” *Proceedings of Micro Electro Mechanical Systems 1993 (MEMS 93)*, pp. 248-253, 1993.
- [15] Todd Thorsen, Sebastian J. Maerkl and Stephen R. Quake, “Microfluidic Large-Scale Integration,” *Science*, vol. 298, pp. 580-584, 2002.
- [16] Kin Fong Lei, Raymond H. W. Lam, Josh H. M. Lam and Wen J. Li, “Polymer Based Vortex Micropump Fabricated by Micro Molding Replication Technique,” accepted in *IEEE/RSJ International Conference on Intelligent Robots and Systems 2004*, Sendai, Japan, September 28 - October 2, 2004.